Corrosion Behavior of Amorphous Sol–Gel TiO$_2$–ZrO$_2$ Nano Thickness Film on Stainless Steel

Lidija Ćurković [1,*] **, Helena Otmačić Ćurković** [2,*] **, Irena Žmak** [1] **, Mihone Kerolli Mustafa** [3] **and Ivana Gabelica** [1]

1   Department of Materials, Faculty of Mechanical Engineering and Naval Architecture, University of Zagreb, 10000 Zagreb, Croatia; irena.zmak@fsb.hr (I.Ž.); ivana.gabelica@fsb.hr (I.G.)
2   Research Laboratory for Corrosion Engineering and Surface Protection, Faculty of Chemical Engineering and Technology, University of Zagreb, 10000 Zagreb, Croatia
3   International Business College Mitrovica, 40000 Mitrovica, Kosovo; m.kerolli@ibcmitrovica.eu
*   Correspondence: lidija.curkovic@fsb.hr (L.Ć.); hotmac@fkit.hr (H.O.Ć.); Tel.: +385-1-616-8183 (L.Ć.); +385-1-4597-117 (H.O.Ć.)

Abstract: In this work, a single-layer TiO$_2$–ZrO$_2$ thin film is deposited on the AISI 316L austenitic stainless steel by the sol–gel process and the dip coating method to improve its corrosion resistance properties. For the sol preparation, titanium isopropoxide and zirconium butoxide are used as the precursors, yttrium acetate hydrate is used for the ZrO$_2$ stabilization, i-propanol as the solvent, nitric acid as the catalyst, acetylacetone as the chelating agent, and the distilled water for the hydrolysis. The deposited films are annealed at 400 °C or 600 °C. Morphology and phase composition of the sol–gel TiO$_2$–ZrO$_2$ films and powders are analyzed by scanning electron microscopy (SEM) equipped with EDX detector and X-ray diffraction (XRD), respectively. The thickness of the sol–gel TiO$_2$–ZrO$_2$ films deposited on the stainless steel is determined by glow discharge optical emission spectrometry (GD-OES). The corrosion behavior of the stainless steel, coated by amorphous films, is evaluated in 3 wt% NaCl and 0.5 mol dm^{-3} HCl by potentiodynamic polarization and electrochemical impedance spectroscopy (EIS) techniques. It is found that the sol–gel TiO$_2$–ZrO$_2$ films with the amorphous structure, deposited by the sol–gel process, and calcined at 400 °C significantly enhance the corrosion properties of AISI 316L in both chloride media.

Keywords: sol–gel; TiO$_2$–ZrO$_2$ films; GD-OES; EIS

1. Introduction

Metals and alloys are some of the most common materials in engineering applications. Therefore, it is very important to recognize the impacts on their service lifetime. One of these influences is corrosion, a destructive process that destroys the metallic structure and causes material failures and structural damage. Special attention is thereby paid to the corrosion behavior of stainless steels [1]. Numerous marine structures and fittings are most often made of stainless steel, because of its comparably good corrosion resistance in sea water, while having high strength and Young's modulus much higher than aluminum alloys. Although stainless steels have major corrosion resistance attributed to the passive oxide film on their surface, there are some environments, like chloride media, that can permanently harm the protective oxide film, leading to localized corrosion. Pitting, stress corrosion, and crevice corrosion may cause structural failure of the stainless steel in chloride media such as sea water. The most widely used stainless steel in a marine environment is AISI 316L, which nevertheless may be susceptible to crevice corrosion in seawater due to unfavorable structural design or manufacturing processes. Crevice corrosion may occur under the deposits, impurities, or in locations where the aggressive chloride medium is retained for a longer period due to poor design solutions [2–5]. Improvement of the stainless steel corrosion resistance can be achieved by the chemical modification of the steel

surface using the corrosion inhibitors, as well as by protective amorphous or crystalline coatings, such as TiO_2, ZrO_2 or SiO_2 thin films or their mixtures [6–9], low-temperature plasma carburizing, nitriding, combined carburizing and nitriding, etc. [10–12]. Ceramic coatings can be deposited on the substrate by several various techniques that have been developed for this purpose. They include physical vapor deposition (PVD), chemical vapor deposition (CVD), electrochemical deposition, thermal spraying, plasma spraying and sol–gel processes, such as spin-, dip- and spray-coating [9,10,13,14]. Among these techniques, sol–gel techniques are often preferred for several reasons: they are simple, low temperature (usually 200 to 600 °C) techniques, which avoid possible decomposition problems; can provide high-purity, high-quality and stoichiometric coatings; the adjustment of the film thickness can be done easily; some of them, like the dip-coating method, are suitable for coatings of complex-shaped substrates, etc. [13,15–17].

To develop and improve the properties of nanostructured thin films, it is necessary to know their surface and depth chemical composition. Useful and well-known analytical techniques which can be used for direct quantitative elemental analysis are Auger electron spectroscopy (AES), X-ray photoelectron spectroscopy (XPS) and secondary ion mass spectrometry (SIMS). Recently, glow discharge optical emission spectrometry (GD-OES), as a very powerful technique for depth profiling analysis of nanolayers, is becoming more popular because of short analysis time, low detection limits, the ability to analyze non-conductive materials, and the quantification of a whole range of chemical elements [6,18–21]. Nanostructured sol–gel TiO_2–ZrO_2 (1:1) films were previously investigated for the improvement of wear resistance of the AISI 304 stainless steel (X5CrNi18-10) substrate [13].

Stainless steel AISI 316L exhibits higher corrosion resistance than AISI 304 against chlorinated solutions, so it is often applied in highly corrosive media like seawater in marine engineering. In general, AISI 316L is not recommended for applications where any hydrochloric acid is present, both because of generalized corrosion as well as localized corrosion, like pitting or crevice corrosion. Hydrochloric acidic solutions are often found in chemical and pharmaceutical industry, where additional protection by coatings is necessary to enable the use and increase the lifetime of stainless steel structural composites and fittings. Ceramic coatings with high chemical resistance are an ideal solution for the application of stainless steels in such media. The goal of this work is the development of an amorphous nanostructured single-layer sol–gel TiO_2–ZrO_2 (1:1) film for the improvement of the localized corrosion protection efficiency (typically, crevice corrosion) of AISI 316L austenitic stainless steel, which is the novelty of this research work. In the present study, an amorphous nanostructured single-layer sol–gel TiO_2–ZrO_2 (1:1) film is deposited on AISI 316L austenitic stainless steel using a dip-coating technique. The elemental composition and the morphology of the annealed TiO_2–ZrO_2 thin films are determined by scanning electron microscopy-energy dispersive X-ray spectroscopy (SEM/EDX) and GD-OES, while the crystallinity of the powdered samples is evaluated by the X-ray diffraction (XRD). The influence of the sol–gel TiO_2–ZrO_2 (1:1) films on the corrosion behavior of the AISI 316L stainless steel is examined in near pH-neutral chloride medium (3 wt% NaCl, to simulate the marine environment) by means of the electrochemical impedance spectroscopy (EIS), and in 0.5 mol dm^{-3} aqueous HCl solution (to simulate aggressive hydrochloric acidic environment) by the potentiodynamic polarization.

2. Materials and Methods

2.1. Substrate

Eighteen (18) steel plates ($10 \times 10 \times 2$ mm^3) are used as substrates: (i) six samples for the linear polarization resistance measurements and the Tafel extrapolation method in 0.5 mol dm^{-3} HCl (three sol–gel TiO_2–ZrO_2 films annealed at 400 °C and three at 600 °C, (ii) six samples for the EIS measurements in 3 wt% NaCl (three sol–gel TiO_2–ZrO_2 films annealed at 400 °C and three at 600 °C), and (iii) six samples for the characterization (GD-OES and SEM/EDX: three sol–gel TiO_2–ZrO_2 films annealed at 400 °C and three at 600 °C) (Figure 1). Therefore, all experiments, for both annealing temperatures,

are performed in triplicate. All data, presented in tables, are expressed as the mean value $\pm$ standard deviation.
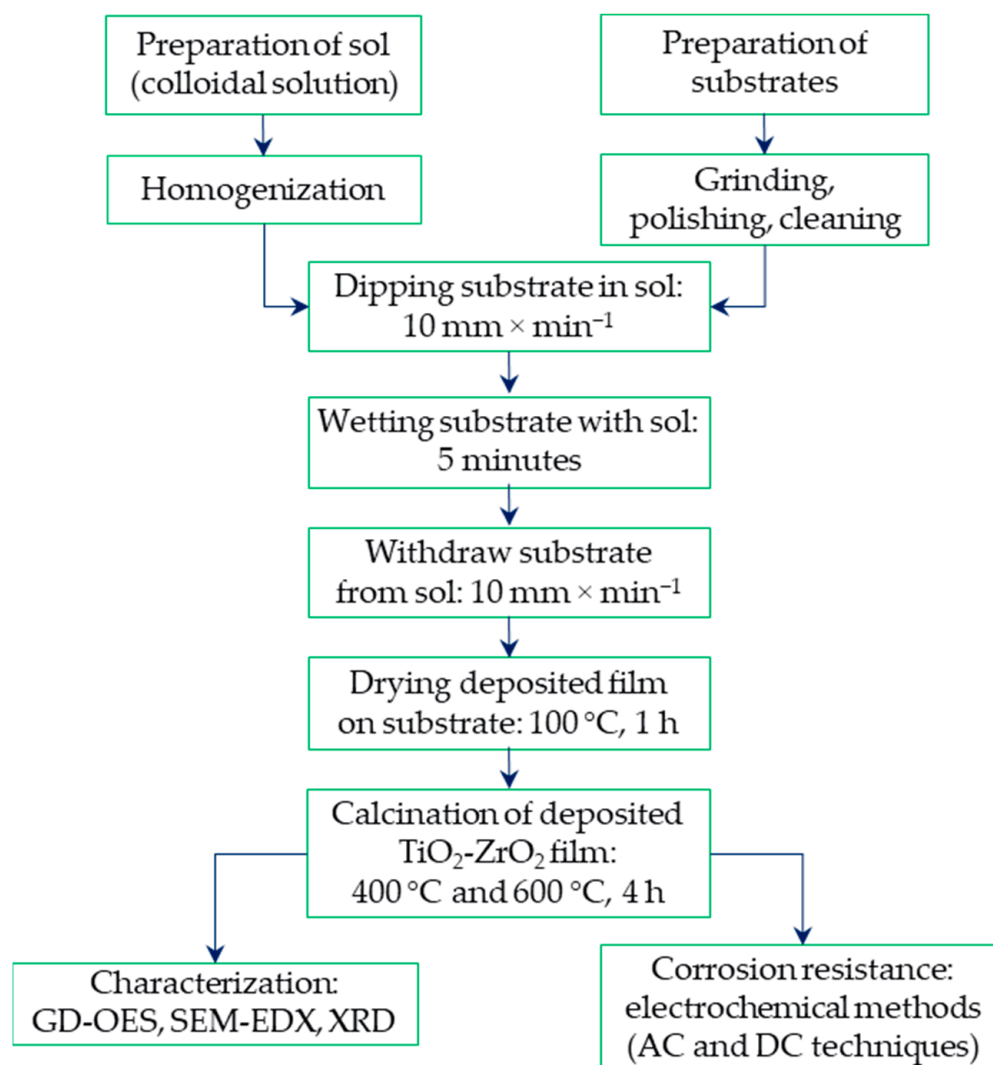

Figure 1. Flow chart for preparation and investigation of sol–gel TiO_2–ZrO_2 films.

Bulk chemical composition of AISI 316L (X2CrNiMo17-12-2, Strojopromet, Šenkovec, Croatia) stainless steel is determined by glow discharge optical emission spectroscopy (GDS 850A, Leco, Saint Joseph, MI, USA) and results in wt% are presented in Table 1.

Table 1. Chemical composition of AISI 316L stainless steel.

					wt%					
C	**P**	**S**	**Si**	**Mn**	**Cu**	**Cr**	**Ni**	**Mo**	**V**	**Fe**
0.026	0.0287	0.0021	0.37	1.42	0.345	16.38	10.53	2.17	0.1	rest

The steel surface is prepared by grinding with various grades of SiC abrasive discs (180 to 1000 grit, Buehler, Essligen, Germany), followed by polishing with the diamond paste (3 μm and 0.25 μm, Buehler, Essligen, Germany). Furthermore, steel substrates are cleaned with the ethanol in an ultrasonic bath (Bransonic 220, Branson Ultrasonics, Danbury, CT, USA), and dried at room temperature prior to the deposition process (Figure 1).

2.2. Chemicals and Reagents

For the preparation of TiO_2–ZrO_2 sol (i.e., colloidal solution) the following chemicals and reagents are used: titanium (IV) isopropoxide ($Ti(OCH(CH_3)_2)_4$, 98%, Sigma–Aldrich, St. Louis, MO, USA), zirconium (IV) butoxide ($Zr(OC(CH3)_3)_4$, 80%, Sigma–Aldrich, St. Louis, MO, USA), yttrium acetate hydrate (($CH_3CO_2)_3Y \times H_2O$, Sigma–Aldrich, St. Louis, MO, USA), i-propyl alcohol (C_3H_7OH, 99.9%, Gram-Mol, Zagreb, Croatia), acetylacetone ($CH_3(CO)CH_2COCH_3$, 99% Merck, Darmstadt, Germany) and nitric acid (HNO_3, 65%, Gram-Mol, Zagreb, Croatia). All chemicals and reagents are analytical grade reagents. The final precursor sol is yellow, transparent, and homogeneous.

2.3. Preparation of Sol–Gel TiO_2–ZrO_2 Film

For the preparation of the sol (colloidal solution), the following components are used:

- 0.5 mol of titanium isopropoxide and 0.5 mol of zirconium butoxide (ratio 1:1) as the precursors;
- 3.75 mmol yttrium acetate hydrate for the ZrO_2 stabilization;
- 0.8 mol acetylacetone as the chelating agent;
- 40 mol of i-propanol as the solvent;
- 0.05 mol of nitric acid as the catalyst;
- 5 mol of distilled water for the hydrolysis.

Stainless steel plates are coated by dip-coating technique using an in-house developed, electrically driven pulley system. The plates are vertically immersed once into the precursor sol with a constant immersion rate of 10 mm $\times$ min^{-1}, left for 5 min in order to allow surface wetting, and withdrawn from the sol using the same rate. After the immersion, the film is dried at room temperature for one hour and subsequently heated at 100 °C for one hour. Finally, the coated steel substrates are calcined in air atmosphere in the furnace P 310 (Nabertherm, Lilienthal, Germany) for 4 h at 400 °C or 600 °C, after being gradually heated in the furnace using a heating rate of 3 °C $\times$ min^{-1}. Finally, the samples are left to cool down to ambient temperature in the furnace (Figure 1).

2.4. Characterization Methods

Thickness measurement and quantitative depth profile (QDP) analysis of sol–gel TiO_2–ZrO_2 films, as well as the bulk chemical analysis of the steel substrate, are carried out by means of GD-OES spectrometer (Leco GDS-850A, Saint Joseph, MI, USA).

Morphological properties and elemental composition of the coatings are studied by scanning electron microscopy with an EDX detector (SEM/EDX, Tescan Vega TS5136LS, Brno-Kohoutovice, Czech Republic).

Part of the sol, remained after the coating deposition on the stainless steel substrates, is dried at 60 °C for 24 h in order to produce dried gels, and annealed for 4 h at 400 °C or 600 °C. To determine the crystallinity of the resulting bulk powdered material, X-ray diffraction (XRD) patterns are recorded on Philips PW 3040/60 X'Pert PRO, AlmeloNetherlands powder diffractometer using CuKα radiation, operating at 45 kV and 40 mA.

2.5. Electrochemical Measurements

The electrochemical behavior of coated and uncoated stainless steel is investigated by means of electrochemical methods (AC and DC techniques, Figure 1). Electrochemical measurements are carried out at room temperature in the conventional three electrode cell, using PAR 263A potentiostat/galvanostat and frequency response analyzer 1025 (both Princeton Applied Research, Oak Ridge, TN, USA). The reference electrode is a saturated calomel electrode (SCE), while a platinum plate is used as the counter electrode.

Electrochemical impedance spectroscopy (EIS) measurements are conducted in a simulated marine environment in near pH-neutral 3 wt% NaCl after 1 h of immersion. Measurements are performed with the amplitude of the voltage perturbation of 0.01 V$_{rms}$ within a frequency range of 100 kHz to 0.01 Hz. All experiments are performed at open circuit potential.

The corrosion resistance of bare and coated stainless steel is also examined in 0.5 mol dm^{-3} HCl by means of the polarization measurements. After one hour of immersion in the prepared solution, the polarization curves are scanned in narrow ($\pm$ 0.02 V vs. open circuit potential) and wide ($\pm$ 0.15 V vs. open circuit potential) potential window. Potential scan rate is 0.166 mV s^{-1}. Data obtained in the narrow potential window are used for the determination of the polarization resistance, i.e., by using the linear polarization method, while the data obtained in the wide potential window are analyzed by the Tafel extrapolation method.

3. Results and Discussion

3.1. Characterization

SEM images and EDX spectra of the single-layered sol–gel TiO$_2$–ZrO$_2$ films obtained after thermal treatment at 400 °C (Figure 2a) or 600 °C (Figure 2b) are presented in Figure 2. In both samples, the surface is completely coated with a thin film that seems homogenous and free from cracks and pinholes. Additionally, the EDX analysis confirms that Zr, Ti and O are present on the surface. Because of the low film thickness, the chemical elements that originate from the steel substrate (especially Fe, Cr and Ni) are also visible in the EDX spectra.
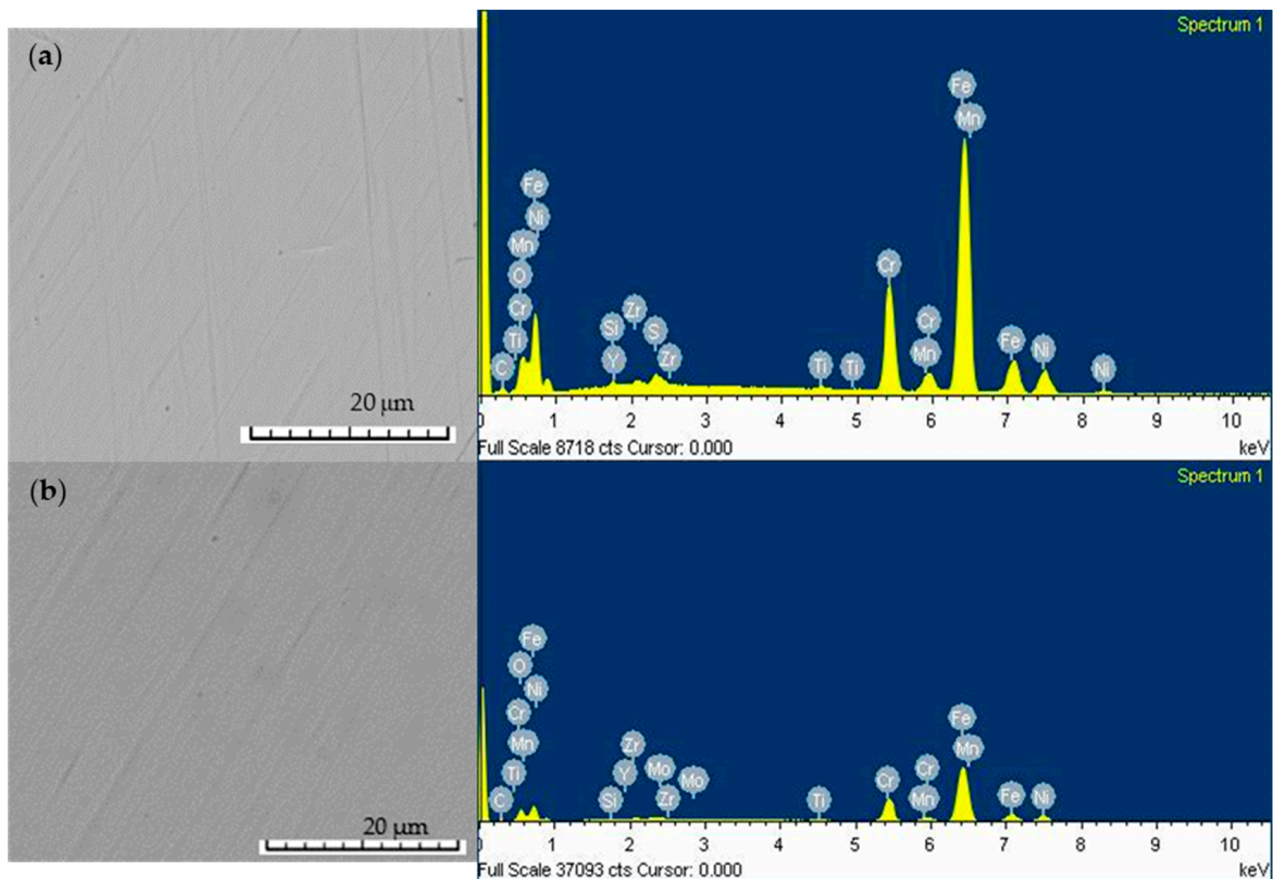

Figure 2. SEM images and EDX spectra of deposited single layer sol–gel TiO$_2$–ZrO$_2$ films on AISI 316L stainless steel: (**a**) annealed at 400 °C; (**b**) annealed at 600 °C.

Figure 3 shows the results of GD-OES depth profile analysis (element atomic percent versus depth) of titanium, zirconium, chromium, nickel and iron in the sol–gel TiO$_2$–ZrO$_2$ films. Since we do not have a photomultiplier to determine the oxygen content, it is not analyzed, but the presence of oxygen is confirmed by SEM/EDX analysis (Figure 2).
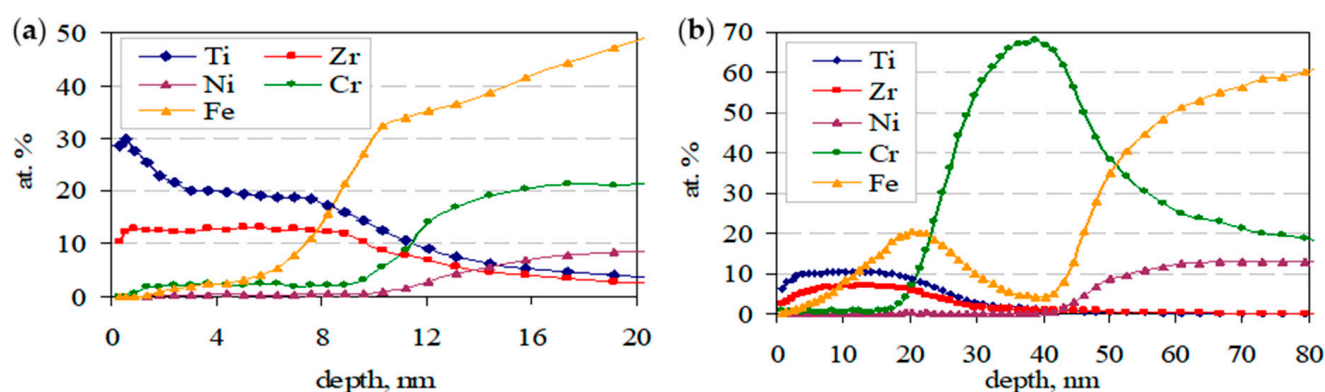
Figure 3. Quantitative depth profile analysis of single layer sol–gel TiO_2–ZrO_2 films on stainless steel obtained by GD-OES: (**a**) annealed at 400 °C; (**b**) annealed at 600 °C.

An approximation of the TiO_2–ZrO_2 films thickness is made based on the depth profile of Ti and Zr, considering the region where the intensities of Ti and Zr are starting to decline and the intensity of Fe or Cr from the substrate becomes significant. The depth profiles indicate that the thickness of the deposited films increases with increasing the calcination temperature. The thickness of the deposited single-layer sol–gel TiO_2–ZrO_2 films is about 8 and 10 nm for films annealed at 400 °C or 600 °C, respectively. The interface between the sol–gel TiO_2–ZrO_2 films and substrates is significantly broadened for films calcined at 600 °C. It is also found that Cr and Fe diffusion from the substrate through the interface and the film depends on the calcination temperature and is more emphasized at a higher temperature.

X-ray diffraction analyses are aimed to obtain structural data for the TiO_2–ZrO_2 system. X-ray diffraction patterns in Figure 4 imply that TiO_2–ZrO_2 powders, annealed at 400 °C or 600 °C, have an amorphous structure. It means that the transformation into the crystalline $ZrTiO_4$, which is expected when the amounts of titania and zirconia are equal, is not yet begun up to the studied temperatures [22,23].
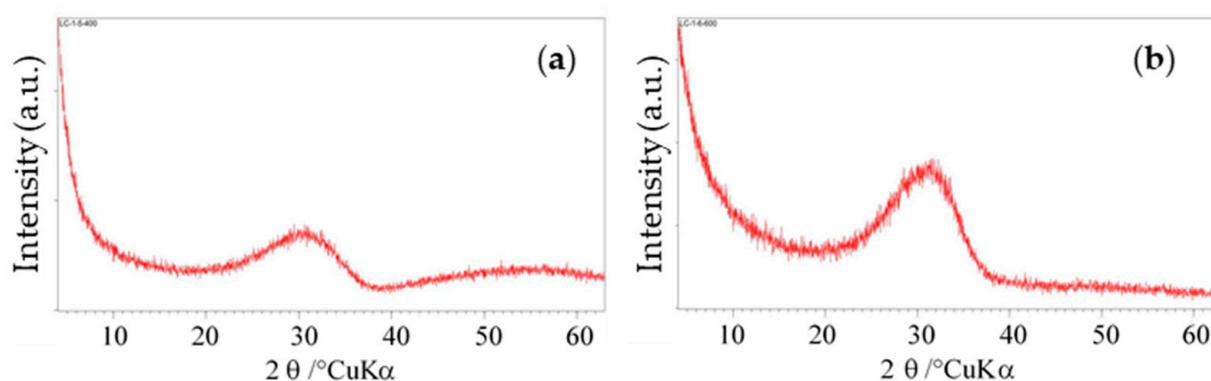

Figure 4. X-ray diffractograms of powdered sol–gel TiO_2–ZrO_2 samples: (**a**) annealed at 400 °C; (**b**) annealed at 600 °C.

3.2. Corrosion Behavior

To examine the protective properties of the nanostructured thin films, coated samples as well as the bare steel are analyzed by electrochemical measurements.

3.2.1. EIS Measurements

Prior to the electrochemical impedance spectroscopy (EIS) measurements, all samples are immersed in 3 wt% NaCl aqueous solution for 1 h to stabilize the system, so that the open-circuit potential (E_{oc}) can be determined. The values of E_{oc} for the uncoated stainless steel sample and the samples coated with sol–gel TiO_2–ZrO_2 films are given in

Table 2. The obtained results show that the presence of the sol–gel TiO$_2$–ZrO$_2$ film on the stainless steel surface shifts the E_{oc} value in the positive direction, which indicates a higher passivation tendency.

Table 2. Values of open-circuit potential (E_{oc}) measured in 3 wt% aqueous NaCl solution (mean value ± standard deviation).

Sample	AISI 316L	TiO$_2$–ZrO$_2$, 400 °C	TiO$_2$–ZrO$_2$, 600 °C
E_{oc}/V vs. SCE	-0.365 ± 0.015	-0.175 ± 0.008	-0.280 ± 0.013

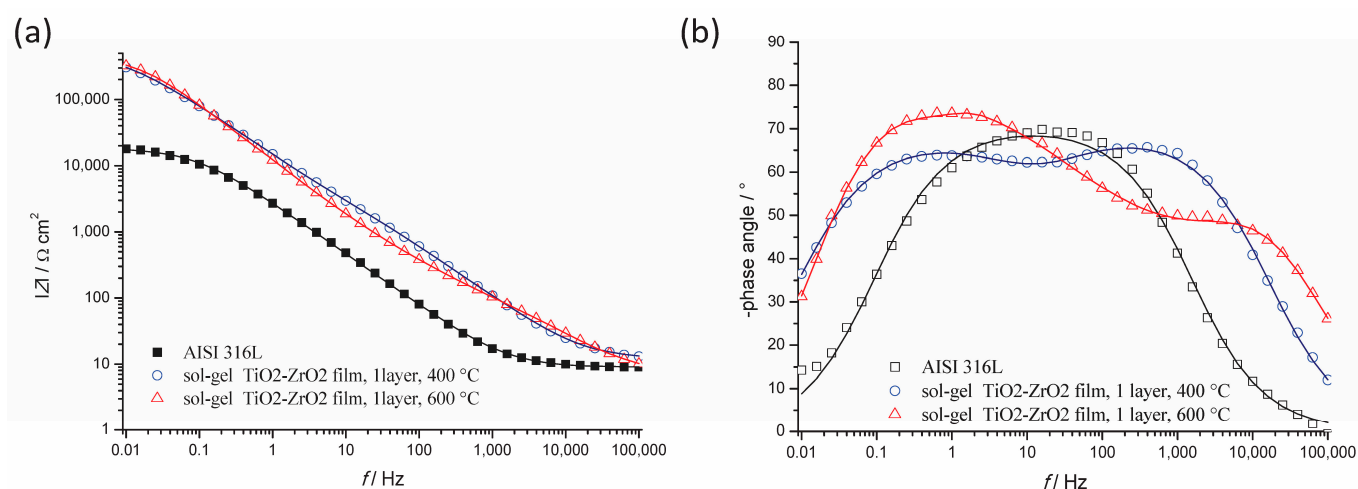The results obtained by the EIS measurements in 3 wt% NaCl are presented in Figure 5.

Figure 5. Bode plot: (**a**) impedance modulus; (**b**) phase angle for uncoated AISI 316L stainless steel and coated with TiO$_2$–ZrO$_2$ films annealed at different temperatures. Markers represent experimental data and lines represent fitted data.

It can be readily seen that the impedance modulus at the lowest frequencies is of one order of magnitude higher for the samples protected by TiO$_2$–ZrO$_2$ films, compared to unprotected stainless steel (Figure 5a). This implies that the corrosion rate of the protected steel is of one magnitude lower than that of the uncoated AISI 316L. From the EIS measurements, it seems that there is not any significant difference in the protective effect between the films calcined at 400 °C or 600 °C. In Figure 5b, it can be seen that for the bare stainless steel only one phase angle maximum appears, indicating the presence of one time constant which is related to the corrosion of steel. On the other hand, two time constants appear on the spectra for the protected steel: one at higher frequencies, representing TiO$_2$–ZrO$_2$ film and another at lower frequencies, corresponding to the corrosion of the steel. The spectra at higher frequencies, obtained for the sample calcined at 400 °C are less depressed than the spectra for the sample calcined at 600 °C.

Impedance spectra for the bare steel are fitted with an equivalent electrical circuit, as presented in Figure 6a. It consists of: R_{el}—the electrolyte resistance, R_{ct}—the charge transfer resistance, Q_{dl}—the constant phase element, representing non-ideal behavior of the electrochemical double layer on the steel surface, and n_{dl}—the associated coefficient. For the spectra of samples with the film annealed at 400 °C it is necessary to use the model with two time constants (Figure 6b). This model contains the additional elements: R_f—the resistance of the pores in the film, Q_f—the constant phase element, describing the coating capacitance, and n_f—the associated coefficient. For the EIS spectra of the samples annealed at 600 °C it is necessary to introduce an additional element to describe the middle frequency region (Figure 6c). This element, hyperbolic tangent diffusion impedance (O) represents

the finite length diffusion inside the pores [24]. The impedance response for finite length diffusion—Z_D is:

$$Z_D = \frac{\tan h\left[K_D(j\omega)^{0.5}\right]}{Y_0(j\omega)^{0.5}} \tag{1}$$

$$K_D = \frac{l}{D} \tag{2}$$

where $j = (-1)^{0.5}$, ω is the angular frequency, l represents pore length and D diffusion coefficient.
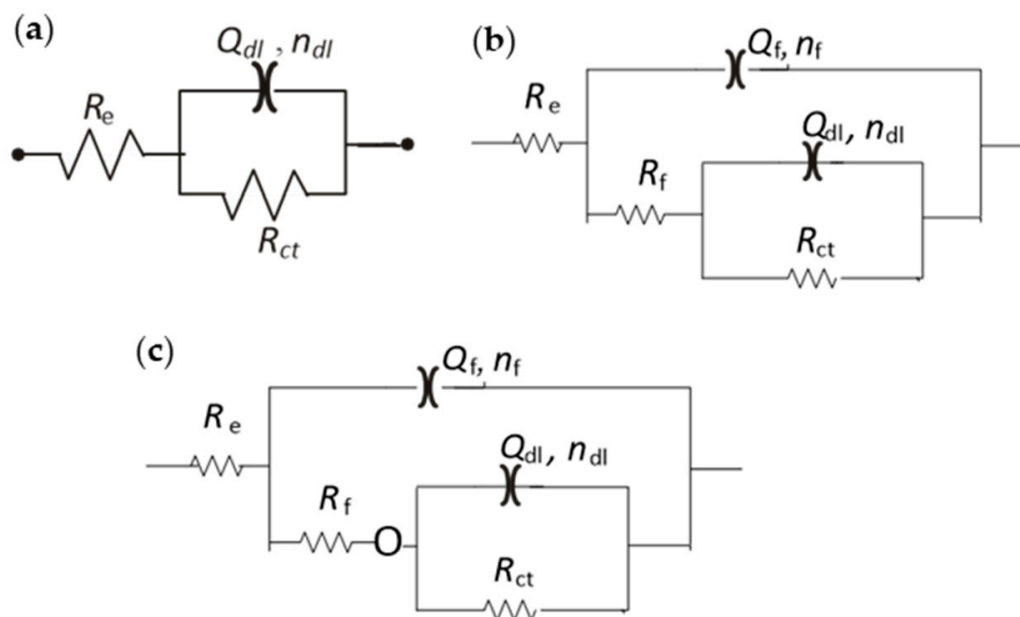

Figure 6. Equivalent electrical circuits used for fitting of EIS spectra for (**a**) bare 316L stain-less steel; (**b**) TiO$_2$–ZrO$_2$ film annealed at 400 °C; (**c**) TiO$_2$–ZrO$_2$ film annealed at 600 °C.

Impedance parameters (Table 3) show that both coatings significantly increased the value of charge transfer resistance (about 20 times) and decreased the value of double-layer capacitance, compared to bare AISI 316L steel. Thus, the corrosion of stainless steel in the pores of the coating is strongly reduced.

Table 3. EIS fitting parameters for bare and coated AISI 316L stainless steel (mean value ± standard deviation) in 3 wt% NaCl.

Sample	AISI 316L	TiO$_2$–ZrO$_2$, 400 °C	TiO$_2$–ZrO$_2$, 600 °C
R_f (Ω cm^2)	-	7485 ± 1147	136 ± 44
Q_f(μSs^n cm^{-2})	-	12.1 ± 3.28	8.89 ± 2.17
n_f	-	0.77 ± 0.12	0.75 ± 0.09
Y_0 (μS s$^{1/2}$ cm^{-2})	-	-	90.1 ± 20.2
K_D (s$^{1/2}$)	-	-	0.77 ± 0.22
R_{ct} (kΩ cm^2)	18.54 ± 2.30	537.0 ± 123.2	459.0 ± 90.6
Q_{dl} (μS s^n cm^{-2})	82.6 ± 10.2	5.96 ± 2.32	8.88 ± 3.61
n_{dl}	0.79 ± 0.05	0.75 ± 0.09	0.98 ± 0.02

It can be observed by examining the parameters for TiO$_2$–ZrO$_2$ films that the film pore resistance value (R_f) is higher for the film annealed at 400 °C than for the film annealed at 600 °C. This could be either due to the thicker or less porous coating. Considering the results of the GD-OES measurements and the values of Q_f (the lower the Q_f, the thicker the coating), which point toward the formation of a thinner film at 400 °C, it may be assumed

that the film formed at lower temperature is less porous than the film formed at 600 °C. The appearance of the diffusion impedance (Y_0 and K_D) for 600 °C film may be related to its higher thickness, which then increases the diffusion path length. The obtained results show that both films efficiently protect the steel surface from corrosion in 3 wt% NaCl.

Previously, EIS measurements in 3% NaCl solution showed a tenfold increase in the charge transfer resistance (R_{ct}) for TiO$_2$ single-layer film [24], i.e., from 3.37 kΩ cm^2 for bare AISI 304 to 32.2 kΩ cm^2 for single layered TiO$_2$ film on the steel substrate. In this work, R_{ct} for the coated steel is twenty times higher than that of the bare stainless steel, i.e., from 18.54 kΩ cm^2 for bare AISI 316L to 537 kΩ cm^2 and 459 kΩ cm^2 after calcination of TiO$_2$–ZrO$_2$ films at 400 or 600 °C, respectively.

3.2.2. Linear Polarization Resistance Measurements

Following one-hour immersion in 0.5 mol dm^{-3} HCl at open circuit potential, linear polarization measurements are performed on the sample of uncoated austenitic stainless steel (AISI 316L) and samples coated with single layer TiO$_2$–ZrO$_2$ film calcined at 400 °C or 600 °C, respectively. The values of polarization resistance, R_p, are calculated from the slopes of E vs. j curves (Figure 7), and together with values of corrosion potential, E_{corr}, and corrosion current densities, j_{corr}, are listed in Table 4. Corrosion current densities are calculated according to the Stern–Geary equation:

$$j_{corr} = \frac{B}{R_P} \tag{3}$$

where the constant B is derived from the anodic and cathodic Tafel slopes (b_a, b_c):

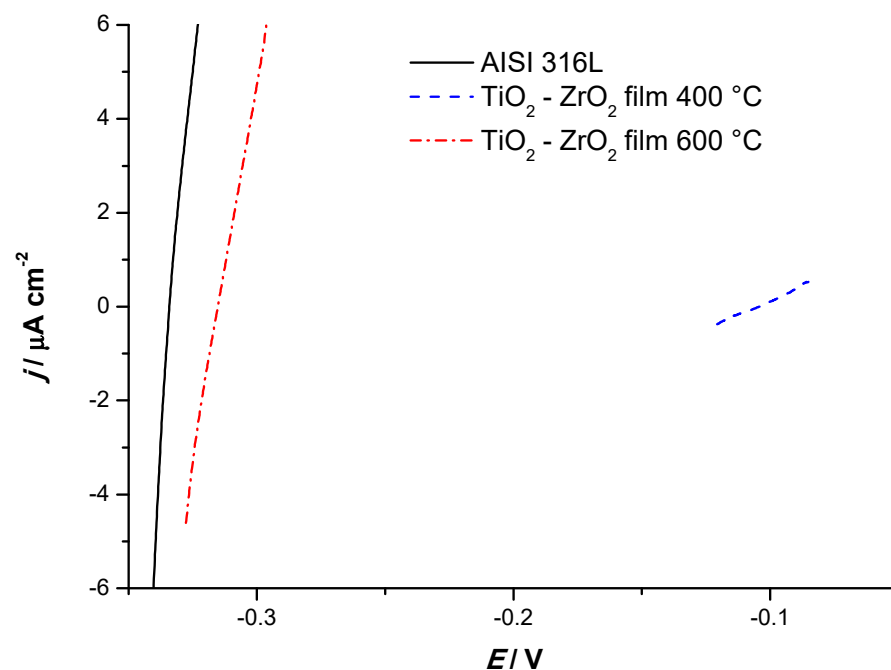$$B = \frac{|b_a \times b_c|}{2.303 \times (b_a + |b_c|)} \tag{4}$$

Figure 7. Polarization curves measured in 0.5 mol dm^{-3} HCl solution for uncoated AISI 316L stainless steel and coated with sol–gel TiO$_2$–ZrO$_2$ film annealed at 400 °C or 600 °C.

Table 4. Values of open-circuit potential (E_{oc}) measured in 0.5 mol dm^{-3} HCl solution (mean value $\pm$ standard deviation).

Sample	E_{corr} vs. SCE, mV	j_{corr}, µA cm^{-2}	R_p, kΩ cm^2
Bare AISI 316L	-351 ± 35	42.11 ± 4.08	1.28 ± 0.16
TiO$_2$–ZrO$_2$ film, 400 °C	-98 ± 20	0.68 ± 0.18	42.30 ± 12.0
TiO$_2$–ZrO$_2$ film, 600 °C	-305 ± 31	8.05 ± 1.39	3.03 ± 0.55

According to Table 4, the coated samples show lower corrosion current density and thus have a higher corrosion resistance in comparison with the unprotected stainless steel. However, the corrosion resistance of the single-coated steel is remarkably reduced with the increase in heat treatment temperature. This means that better corrosion properties in 0.5 mol dm^{-3} HCl medium reveals the coated steel substrate annealed at 400 °C. Regarding the E_{corr} in 0.5 mol dm^{-3} HCl, it may be observed that the most noble values are obtained for the film annealed at 400 °C. A similar phenomenon is observed for E_{oc} values in neutral medium. The values of the corrosion potential of the samples annealed at 600 °C are closer to that of the unprotected AISI 316L steel. This is in accordance with our previous conclusions, that at 600 °C a more porous coating is formed. The higher the porosity of the coating, the closer the corrosion potential of the coated sample to that of the substrate, which is clearly observed in lower polarization resistance, R_p, Table 4. This effect is more pronounced in acidic than in neutral medium, which may be related to its higher corrosivity. The achieved increment in the polarization resistance is better than those found in the literature for the steel protected by monolithic (Al$_2$O$_3$, SiO$_2$, ZrO$_2$) and composite (SiO$_2$–TiO$_2$, SiO$_2$–Al$_2$O$_3$) sol–gel nanostructured ceramic films [25–27]. For example, in our previous work [24], TiO$_2$ films on AISI 304 were examined in the same media; however, the corrosion protection by the three-layer TiO$_2$ film was lower than the protection observed in this work. Previously, a ninefold decrease in corrosion current density in 0.5 mol dm^{-3} HCl solution was obtained for TiO$_2$ films compared to bare AISI 304 steel, i.e., from 64.85 µA cm^{-2} to 7.77 µA cm^{-2}. In this work, a sixfold decrease in corrosion current is observed for the single-layer TiO$_2$–ZrO$_2$ film, i.e., from 42.11 µA cm^{-2} to 0.68 µA cm^{-2} when the film is calcined at 400 °C. When the coating is calcined at 600 °C, corrosion current is 8.05 µA cm^{-2}.

Studies conducted by de Lima Neto et al. [25] on ZrO$_2$ coating on AISI 316L steel in 0.5 mol dm^{-3} H$_2$SO$_4$ showed only a tenfold decrease in the corrosion current density.

3.2.3. Tafel Extrapolation Method

The potentiodynamic polarization curves of the bare and the coated stainless steel obtained in 0.5 mol dm^{-3} HCl are shown in Figure 8. The corrosion parameters: the corrosion potential (E_{corr}), the corrosion current density (j_{corr}), and the anodic and cathodic Tafel slopes (b_a, b_c) are determined from the polarization curves by the Tafel extrapolation method. The corresponding data are summarized in Table 5.
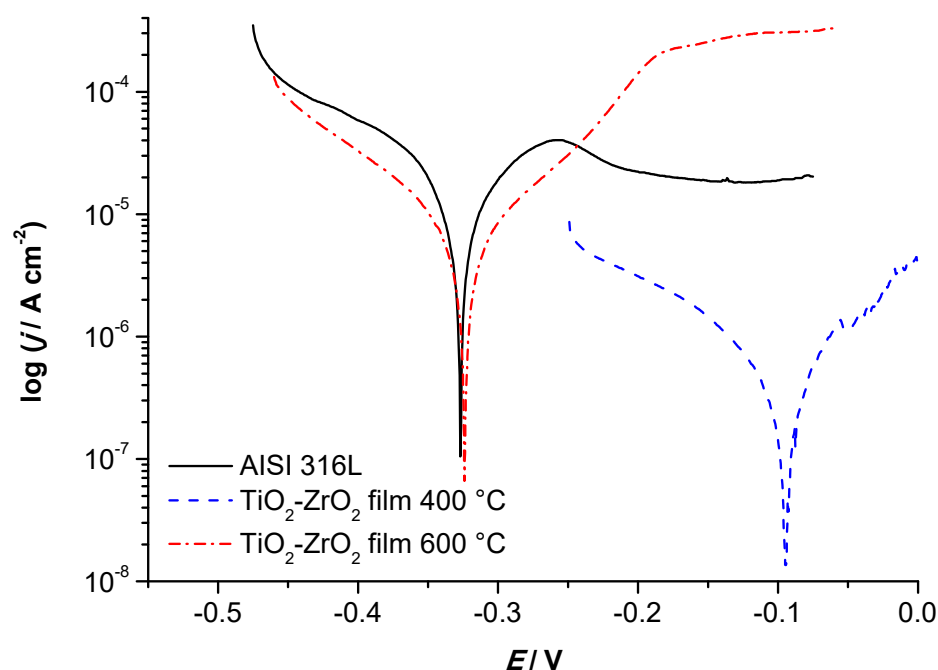
Figure 8. Potentiodynamic curves of bare AISI 316L stainless steel and steel with TiO_2–ZrO_2 film annealed at 400 °C or 600 °C, measured in 0.5 mol dm^{-3} HCl solution.

Table 5. Electrochemical parameters obtained from potentiodynamic polarization curves measured in 0.5 mol dm^{-3} HCl solution (mean value ± standard deviation).

Sample	E_{corr} vs. SCE, mV	j_{corr}, µA/cm²	b_a, mV/dec	$-b_c$, mV/dec
Bare AISI 316L	-336 ± 38	40 ± 3.15	280 ± 44	180 ± 31
TiO_2–ZrO_2 film, 400 °C	-95 ± 24	0.65 ± 0.10	130 ± 20	140 ± 27
TiO_2–ZrO_2 film, 600 °C	-304 ± 40	9.35 ± 1.51	105 ± 19	140 ± 25

From the results of the Tafel extrapolation method, it can be concluded that TiO_2–ZrO_2 film annealed at 400 °C shifts the corrosion potential of bare stainless steel in the positive direction by approximately 240 mV. With the increase in coating treatment temperature from 400 to 600 °C, the corrosion potential becomes close to that of the uncoated stainless steel. A similar trend is observed for the values of the corrosion current density (j_{corr}). Compared to the bare stainless steel, the corrosion current density decreases about 67 times when the annealing temperature is 400 °C, and only 4 times when the coating is calcined at 600 °C.

These results confirm that the application of the sol–gel TiO_2–ZrO_2 films calcined at 400 °C significantly increases the corrosion resistance of the stainless steel. Regarding the influence of the coating on the Tafel coefficients, b_a and b_c, it appears that b_c is not changed significantly, while a decrease in b_a is observed for the coated samples, which indicates that the anodic reaction on the coated samples is mainly under the activation control.

Studies in both acid and neutral chloride solutions show that better corrosion protection is achieved by TiO_2–ZrO_2 coating calcined at 400 °C than the same coating calcined at 600 °C. Results of electrochemical studies indicate that this is related to the higher porosity of the latter coating, but it may also be related to an enhanced diffusion of the elements from the substrate into the coating at elevated temperatures. It can be observed from Figure 3 that at 400 °C the outer coating layer contains similar amounts of Cr and Fe, while the outer part of the coating heated at 600 °C contains much more Fe than Cr. As the corrosion resistance of Fe is much lower than that of Cr, a higher corrosion rate of the system containing more Fe is understandable.

4. Conclusions

Nanostructured sol–gel TiO_2–ZrO_2 films are deposited on the stainless steel AISI 316L (X2CrNiMo17-12-2) substrate by the dip-coating method. For the sol preparation, titanium isopropoxide and zirconium butoxide is used as the precursors, i-propanol as the solvent, nitric acid as the catalyst, acetylacetone for the peptization, and the distilled water for the hydrolysis.

Deposited sol–gel TiO_2–ZrO_2 films after thermal treatment at 400 °C or 600 °C are characterized by SEM/EDX, GD-OES, XRD and electrochemical measurements. From the obtained results, the following conclusion can be drawn:

- Nano-thickness of TiO_2–ZrO_2 films after thermal treatment at 400 °C or 600 °C are 8 nm and 10 nm, respectively.
- XRD analysis confirms that the sol–gel TiO_2–ZrO_2 powdered samples have an amorphous structure.
- The results of the quantitative depth profile analysis of the sol–gel TiO_2–ZrO_2 films deposited on the stainless steel, obtained by glow-discharge optical emission spectrometry (GD-OES), indicate that the thickness of the deposited film increases by increasing the calcination temperature. It is also found that the diffusion of some chemical elements (Cr and Fe) from the substrate into the deposited films increases by increasing the heat treatment temperature. GD-OES, as a fast, easy-to-use analytical technique, is proven to be a powerful tool for a rapid bulk chemical analysis, as well as for the determination of elemental concentrations as a function of the depth, measured in the nanoscale.
- The results of the electrochemical tests (AC and DC methods) show that the sol–gel TiO_2-ZrO_2 film annealed at 400 °C significantly improves the corrosion resistance of the austenitic stainless steel AISI 316L in acidic and neutral chloride medium, compared to bare steel and to films annealed at 600 °C.
- Composite TiO_2–ZrO_2 coating provides better corrosion protection than monolithic TiO_2 films that were examined in previous work [24] on AISI 304 in the same media. A previous study in 3% NaCl solution showed an increase in the charge transfer resistance from 3.37 kΩ cm^2 for uncoated AISI 304 to 32.2 kΩ cm^2 for TiO_2 film-protected steel. In this work, R_{ct} is increased from 18.54 kΩ cm^2 for bare AISI 316L to 537 kΩ cm^2 or 459 kΩ cm^2 in TiO_2–ZrO_2 films calcined at 400 or 600 °C, all measured in 3% NaCl solution, which simulates the marine environment. This shows that single-layered sol–gel TiO_2–ZrO_2 coating significantly improves the corrosion resistance of AISI 316L stainless steel for the application in marine engineering.
- Previous study [24] of corrosion resistance of AISI 304, protected with TiO_2 film, measured in 0.5 mol dm^{-3} HCl solution, showed a reduction in corrosion current density from 64.85 µA cm^{-2} to 7.77 µA cm^{-2}. Presented research shows an extensive reduction in corrosion current from 42.11 µA cm^{-2} for unprotected AISI 316L to 0.68 µA cm^{-2} for AISI 316L coated with a single-layer of TiO_2-ZrO_2 calcined at 400 °C. When the TiO_2-ZrO_2 is calcined at 600 °C, the corrosion current is also significantly lower, 8.05 µA cm^{-2}. These findings suggest that although the stainless steel AISI 316L is typically not recommended for the application where any hydrochloric acid media is present, its corrosion resistance may be significantly improved by TiO_2-ZrO_2 sol–gel coating calcined at 400 °C.
- Electrochemical studies show that the differences in corrosion protection level provided by films annealed at 400 °C or 600 °C can be related to the increased porosity of the coating treated at 600 °C. Thus, an increase in the annealing temperature is not recommended for TiO_2–ZrO_2 films preparation. Further research should, rather, focus on the possibility of application of several layers of TiO_2–ZrO_2 films as a means of additional improvement of the stainless steel corrosion protection.

References

1. Rezaee, S.; Arman, A.; Jurečka, S.; Grayeli Korpi, A.; Mwema, F.; Luna, C.; Sobola, D.; Kulesza, S.; Shakoury, R.; Bramowicz, M.; et al. Effect of annealing on the micromorphology and corrosion properties of Ti/SS thin films. *Superlattices Microstruct.* **2020**, *146*, 106681. [CrossRef]

2. Yu, J.; Ji, G.; Liu, Q.; Zhang, J.; Shi, Z. Effect of sol–gel ZrO_2 films on corrosion behavior of the 304 stainless steel in coal-gases environment at high temperature. *Surf. Coat. Technol.* **2017**, *331*, 21–26. [CrossRef]

3. Coelho, L.B.; Kossman, S.; Mejias, A.; Noirfalise, X.; Montagne, A.; Van Gorp, A.; Poorteman, M.; Olivier, M.G. Mechanical and corrosion characterization of industrially treated 316L stainless steel surfaces. *Surf. Coat. Technol.* **2020**, *382*, 125175. [CrossRef]

4. Kim, J.J.; Young, M.Y. Study on the Passive Film of Type 316 Stainless Steel. *Int. J. Electrochem. Sci.* **2013**, *8*, 11847–11859.

5. Bačić, I.; Otmačić Ćurković, H.; Ćurković, L.; Mandić, V.; Šokčević, Z. Corrosion Protection of AISI 316L Stainless Steel with the Sol–Gel Yttria Stabilized ZrO_2 Films: Effects of Sintering Temperature and Doping. *Int. J. Electrochem. Sci.* **2016**, *11*, 9192–9205. [CrossRef]

6. Kossman, S.; Bertolucci Coelho, L.; Montagne, A.; Mejias, A.; Van Gorp, A.; Coorevits, T.; Touzin, M.; Druart, M.-E.; Staia, M.H.; Poorteman, M.; et al. The effect of the substrate surface state on the morphology, topography and tribocorrosion behavior of Si/Zr sol–gel coated 316L stainless steel. *Surf. Coat. Technol.* **2021**, *406*, 12666. [CrossRef]

7. Saman Khosravi, H.; Veerapandiyan, K.V.; Vallant, R.; Reichmann, K. Effect of processing conditions on the structural properties and corrosion behavior of TiO_2–SiO_2 multilayer coatings derived via the sol–gel method. *Ceram. Int.* **2020**, *46*, 17741–17751. [CrossRef]

8. Fotovvati, B.; Namdari, N.; Dehghanghadikolaei, A. On Coating Techniques for Surface Protection: A Review. *J. Manuf. Mater. Process.* **2019**, *3*, 28. [CrossRef]

9. Mazur, A.; Szczurek, A.; Chęcmanowski, J.G.; Szczygieł, B. Corrosion resistance and bioactivity of SiO_2-Y_2O_3 coatings deposited on 316L steel. *Surf. Coat. Technol.* **2018**, *50*, 502–510. [CrossRef]

10. Adachi, S.; Ueda, N. Wear and corrosion properties of cold-sprayed AISI 316L coatings treated by combined plasma carburizing and nitriding at low temperature. *Coatings* **2018**, *8*, 456. [CrossRef]

11. Adachi, S.; Egawa, M.; Yamaguchi, T.; Ueda, N. Low-temperature plasma nitriding for austenitic stainless steel layers with various nickel contents fabricated via direct laser metal deposition. *Coatings* **2020**, *10*, 365. [CrossRef]

12. Shi, W.; Wang, J.; Jiang, R.; Xiang, S. Anticorrosion Properties of the Low-Temperature Glow Plasma Nitriding Layer on AISI 904L Austenitic Stainless Steel in Hydrofluoric Acid Obtained at Various NH_3 Pressures. *Coatings* **2020**, *12*, 1156. [CrossRef]

13. Grilec, K.; Ćurković, L.; Žmak, I. Wear rate evaluation of sol–gel TiO_2-ZrO_2 films by quantitative depth profile analysis. *Trans. FAMENA* **2020**, *44*, 1–11. [CrossRef]

14. Sakoman, M.; Ćorić, D.; Aleksandrov Fabijanić, T.; Kovačić, S. Tribological Properties of Coatings Applied on Near-Nano and Nanostructured WC-Co Hardmetals by Using Plasma- Assisted Chemical Vapour Deposition Technique. *Trans. FAMENA* **2020**, *44*, 29–42. [CrossRef]

15. Metroke, T.L.; Parkhill, R.L.; Knobbe, E.T. Passivation of metal alloys using sol–gel-derived materials—A review. *Prog. Org. Coat.* **2001**, *41*, 233–238. [CrossRef]

16. Gheriani, R.; Chtourou, R. Preparation of Nanocrystalline Titanium Dioxide (TiO_2) Thin Films by the Sol–Gel Dip Coating Method. *J. Nano Res.* **2012**, *16*, 105–111. [CrossRef]

17. Zhang, H.; Wang, C.; Xue, B.; Luo, J. Effect of Sol–Gel Film on the Corrosion Resistance of Low Carbon Steel Plate. *Mater. Sci. Forum* **2020**, *984*, 174–177. [CrossRef]

18. Seah, M.P.; Mulcahy, C.P.A.; Biswas, S. Nonlinearities in depth profiling nanometer layers. *J. Vac. Sci. Technol. B* **2010**, *28*, 1215–1221. [CrossRef]

19. Escobar, R.G.; Gago, R.; Duday, D.; Palacio, C. Towards nanometric resolution in multilayer depth profiling: A comparative study of RBS, SIMS, XPS and GDOES. *Anal. Bioanal. Chem.* **2010**, *396*, 2725–2740. [CrossRef] [PubMed]

20. Xhoffer, C.; Dillen, H. The Versatility of GDOES: From Bulk Analysis to Thin Film and Surface Analysis. *BHM Berg-Und Hüttenmännische Mon.* **2007**, *152*, 18–23. [CrossRef]
21. Nelis, T.; Pallosi, J. Glow Discharge as a Tool for Surface and Interface Analysis. *Appl. Spectrosc. Rev.* **2006**, *41*, 227–258. [CrossRef]
22. Manriquez, M.E.; Picquart, M.; Bokhimi, X.; López, T.; Quintana, P.; Coronado, J.M. X-Ray Diffraction, and Raman Scattering Study of Nanostructured ZrO_2-TiO_2 Oxides Prepared by Sol–Gel. *J. Nanosci. Nanotechnol.* **2008**, *8*, 6623–6629. [CrossRef]
23. Liang, L.; Sheng, Y.; Xu, Y.; Wu, D.; Sun, Y. Optical properties of sol gel derived ZrO_2-TiO_2 composite films. *Thin Solid Films* **2007**, *515*, 7765–7771. [CrossRef]
24. Ćurković, L.; Otmačić Ćurković, H.; Salopek, S.; Majić Renjo, M.; Šegota, S. Enhancement of corrosion protection of AISI 304 stainless steel by nanostructured sol–gel TiO_2 films. *Corros. Sci.* **2013**, *77*, 176–184. [CrossRef]
25. De Lima Neto, P.; Atik, M.; Avaca, L.A.; Aegerter, M.A. Sol-Gel Coatings for Chemical Protection of Stainless Steel. *J. Sol-Gel Sci. Technol.* **1994**, *2*, 529–534. [CrossRef]
26. Ruhi, G.; Modi, O.P.; Sinha, A.S.K.; Singh, I.B. Effect of sintering temperatures on corrosion and wear properties of sol–gel alumina coatings on surface pre-treated mild steel. *Corros. Sci.* **2008**, *50*, 639–649. [CrossRef]
27. Atik, M.; Kha, C.R.; de Lima Neto, P.; Avaca, L.A.; Aegerter, M.A.; Zarzycki, J. Protection of 316L stainless steel by zirconia sol–gel coatings in 15% H_2SO_4 solutions. *J. Mater. Sci. Lett.* **1995**, *14*, 178–181. [CrossRef]